Supporting Information

S1. Evolution of record-breaking temperatures in a stationary climate

The theory states that in a stationary climate, and for a sequence of independent identically distributed random variables, the number of records is theoretically expected to decrease with time. At year n, the probability for a record to occur is $1/n$ (Glick 1978; Benestad 2003). To mask this inherent decrease with time and to better visualize the trends in record occurrence we use the normalized form: each year the number of records is multiplied by n. Under this normalized form, the expected number of records in a stationary climate is constant and always equal to 1.

Numerous studies (e.g. Meehl et al. 2009; Elguindi et al. 2012; Wergen et al. 2013 among others) have shown that until the 1980-1990s, the record evolution oscillated around this theoretical decay in 1/n according to natural fluctuations (interannual to multi-decadal variations; see Bador et al. 2015a for more details). From the 1980-1990s onwards we observe a change in the record evolution, with an increase in the number of warm records and a decrease in the number of cold records. These changes result in a shift from this theoretical record evolution expected in a stationary climate. In this study, we compare the simulated historical and future number of records to 1, the theoretical number of records expected in a stationary climate which is consistent with the beginning of the observations.

S2. Spatial clustering of extreme events

The clustering algorithm originates from the multivariate extreme value theory (Coles 2001; Beirlant et al. 2004; de Haan and Ferreira 2006; Resnik 2007) and is thus perfectly recommended to extract homogenized spatial patterns from series of extreme temperatures (Bador et al. 2015b) or heavy precipitations (Bernard et al. 2013) for instance. The clustering algorithm is applied to the SQR observations over the period with maximum and consistent station data availability (1980-2010, see figure S1). Details of the methodology can be found in Bernard et al. (2013) but the main tools are presented below.

First, the proximity of two stations has to be evaluated. To that end, no geographical information is taken into account but only time series of Tmax summer maxima. The spatial dependence among the time series is evaluated using a rank-based distance (Cooley et al. 2006) based on the comparison of the ordering between two series. This rank-based distance is adapted from the variogram distance often used in geostatistics (Wackernagel 2003) and is defined by $\hat{d}_{ij} = \frac{1}{2T}\sum_{t=1}^{T}|R_i^{(t)} - R_j^{(t)}|$ where $R_i^{(t)}$ corresponds to the rank of the t-th year within the time series of maxima.

Secondly, the stations have to be compared to each other in order to be gathered in a K number of clusters specified as input. The clustering algorithm used here is the Partitioning Around Medoids algorithm (PAM; Kaufman and Rousseeuw 1990). It divides our set of N stations into K clusters and is appropriate for extremes as averaging is not required (contrary to the well-known k-means algorithm). The algorithm selects one of the time series as the cluster center, named medoid. This medoid can be understood as the station whose time series of seasonal maxima best represents its cluster.

Finally, the robustness of the affiliation of a station into a cluster is evaluated using the silhouette coefficient (Rousseeuw 1986), defined by $s_i(K) = 1 - \frac{d_{ik}}{\delta_{i,-k}}$, where d_{ik} represents the intra-cluster distance between the medoid k and the station i, and $\delta_{i,-k}$ corresponds to the smallest distance between station i and all the other medoids except for k. In other words, the silhouette coefficient measures the proximity of a station to its medoids and in the same time the distance to its nearest neighbor's medoid. Hence, stations with too low coefficient value will not be considered as significant ($sil.coef. < 0.5$; see figure 1). Similarly, the robustness of a cluster can be assessed using the averaged silhouette coefficient, i.e. the mean value of the silhouette coefficients of its significant stations.

References

- Bador, M., Terray, L., & Boé, J. (2015a). Detection of anthropogenic influence on the evolution of record‐breaking temperatures over Europe. Climate Dynamics, 46(9), 2717–2735.

- Bador, M., Naveau, P., Gilleland, E., Castellà, M., & Arivelo, T. (2015b). Spatial clustering of summer temperature maxima from the CNRM-CM5 climate model ensembles & E-OBS over Europe. Weather and Climate Extremes, Volume 9, September 2015, Pages 17-24.

- Benestad, R. E. (2003). How often can we expect a record event? Climate Research, 25(iid), 3–13.

- Beirlant, J., Goegebeur, Y., Segers, J., & Teugels, J. (2004). Statistics of extremes: Theory and applications. John Wiley & Sons: New York.

- Bernard, E., Naveau, P., Vrac, M., & Mestre, O. (2013). Clustering of Maxima: Spatial Dependencies among Heavy Rainfall in France. Journal of Climate, 26(20), 7929–7937.

- Coles, S., Bawa, J., Trenner, L., & Dorazio, P. (2001). An introduction to statistical modeling of extreme values (Vol. 208). London: Springer.

- Cooley, D., Naveau, P., & Poncet, P. (2006). Dependence in Probability and Statistics. In P. D. P. Bertail & P. Soulier (Eds.) (Vol. 187, pp. 373–390). inbook, New York, Springer.

- Elguindi, N., Rauscher, S. a., & Giorgi, F. (2012). Historical and future changes in maximum and minimum temperature records over Europe. Climatic Change, 117(1–2), 415–431.

- Glick, N. E. D. (1978). Breaking records and breaking boards. American Mathematical Monthly, 85, 2–26.

- de Haan, L., & Ferreira, A. (2006). Extreme Value Theory, An Introduction. Springer Series in Operations Research and Financial Engineering.

- Kaufman, L., & Rousseeuw, P. J. (1990). Finding Groups in Data: An Introduction to Cluster Analysis. book, Wiley, New-York.

- Meehl, G. a., Tebaldi, C., Walton, G., Easterling, D., & McDaniel, L. (2009). Relative increase of record high maximum temperatures compared to record low minimum temperatures in the U.S. Geophysical Research Letters, 36(23), L23701.

- Resnick, S. I. (2007). Heavy-Tail Phenomena: Probabilistic and Statistical Modeling. Springer Series in Operations Research and Financial Engineering.

- Rousseeuw, P. J. (1986). Silhouettes: a graphical aid to the interpretation and validation of cluster analysis. J. Comp App Math, 20(53–65).

- Wackernagel, H. (2003). Multivariate Geostatistics. An Introduction with Applications (3rd ed.). book, Heidelberg: Springer.

- Wergen, G., Hense, A., & Krug, J. (2014). Record occurrence and record values in daily and monthly temperatures. Climate dynamics, 42(5-6), 1275-1289.

Supporting Table and Figures

Supplementary Table: List of the CMIP5 model names and institution.

	Model name	Institution
1	BCC-CSM1.1M	BCC
2	BNU-ESM	GCESS
3	CanESM2	CCCma
4	CMCC-CESM	CMCC
5	CMCC-CM	CMCC
6	CMCC-CMS	CMCC
7	CNRM-CM5	CNRM-CERFACS
8	ACCESS1-0	CSIRO-BOM
9	CSIRO-Mk3-6-0	CSIRO-QCCCE
10	INM-CM4	INM
11	IPSL-CM5A-LR	IPSL
12	IPSL-CM5A-MR	IPSL
13	IPSL-CM5B-LR	IPSL
14	FGOALS-g2	LASG-CESS
15	MIROC5	MIROC
16	MIROC-ESM	MIROC
17	MIROC-ESM-CHEM	MIROC
18	HadGEM2-CC	MOHC
19	HadGEM2-ES	MOHC
20	MPI-ESM-MR	MPI-M
21	MPI-ESM-LR	MPI-M
22	CCSM4	NCAR
23	NorESM1-M	NCC
24	HadGEM2-AO	NIMR/KMA
25	GFDL-CM3	NOAA GFDL
26	GFDL-ESM2G	NOAA GFDL
27	GFDL-ESM2M	NOAA GFDL
28	CESM1-BGC	NFS-DOE-NCAR
29	CESM1-CAM5	NFS-DOE-NCAR

Figure S1: (a) Map of the observed current (in 2005) summer record maximum values in France and **(b)** its yearly evolution (one line per station, ordered by increasing altitude as represented by the black line on the right side). Records are calculated from the longest possible time series for each station. The location of the maximum in France is indicated by a star and its value is given next to it in (a). The observed 2003 heatwave is marked in red in (b).
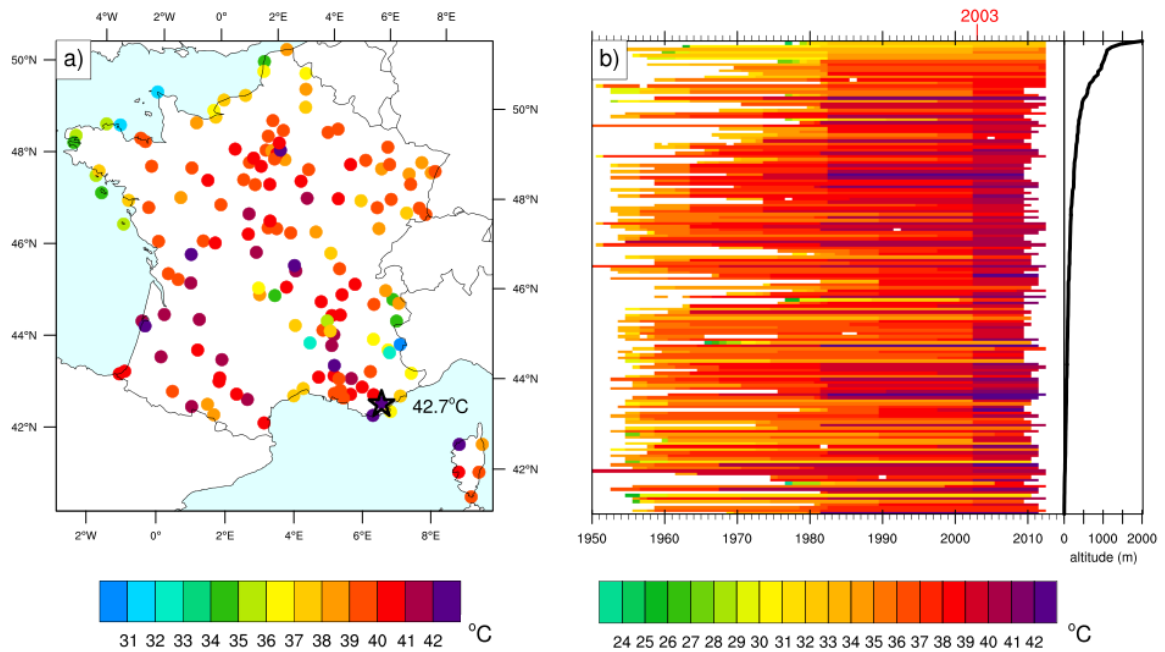
Figure S2: Same as figure 1 for different numbers of cluster (K).
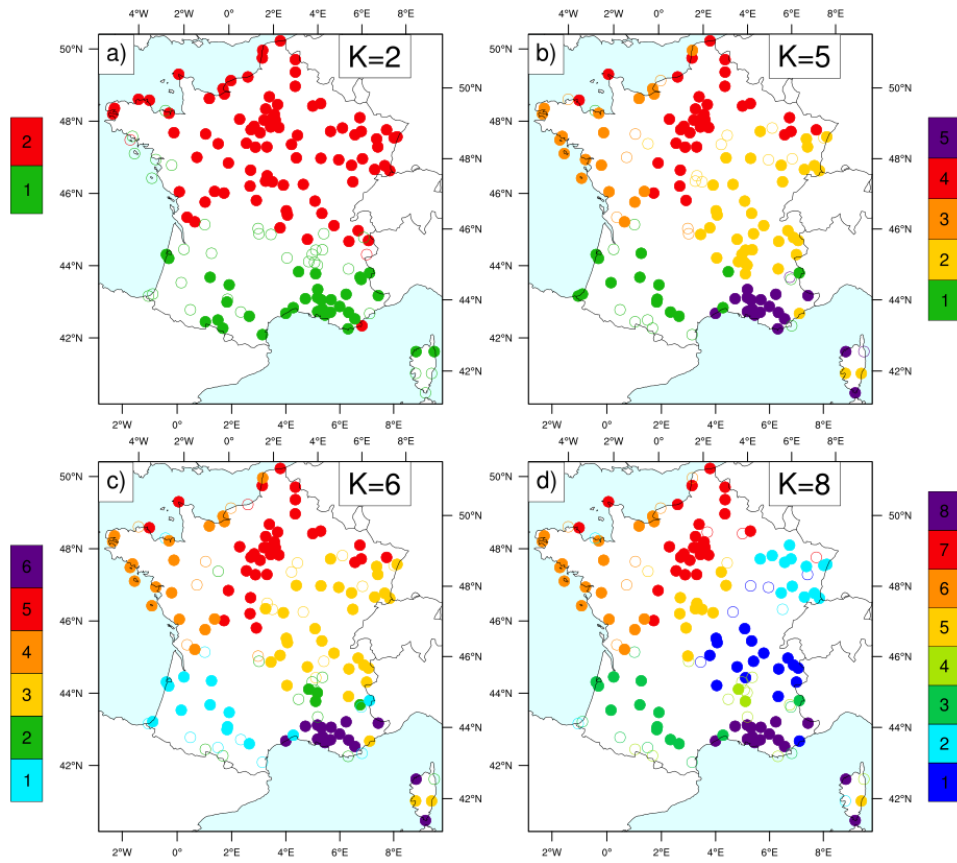
Figure S3: Map of the year when the summer record maximum value is reached, as simulated by ALADIN-SCEN. Symbols refer to the five regions given by the clustering algorithm (figure 1). Symbols are centered on the closest ALADIN grid point to each station (shown by a solid circle). The relative number of stations whose record maximum value was reached in 2075 is indicated in the bottom-left box.
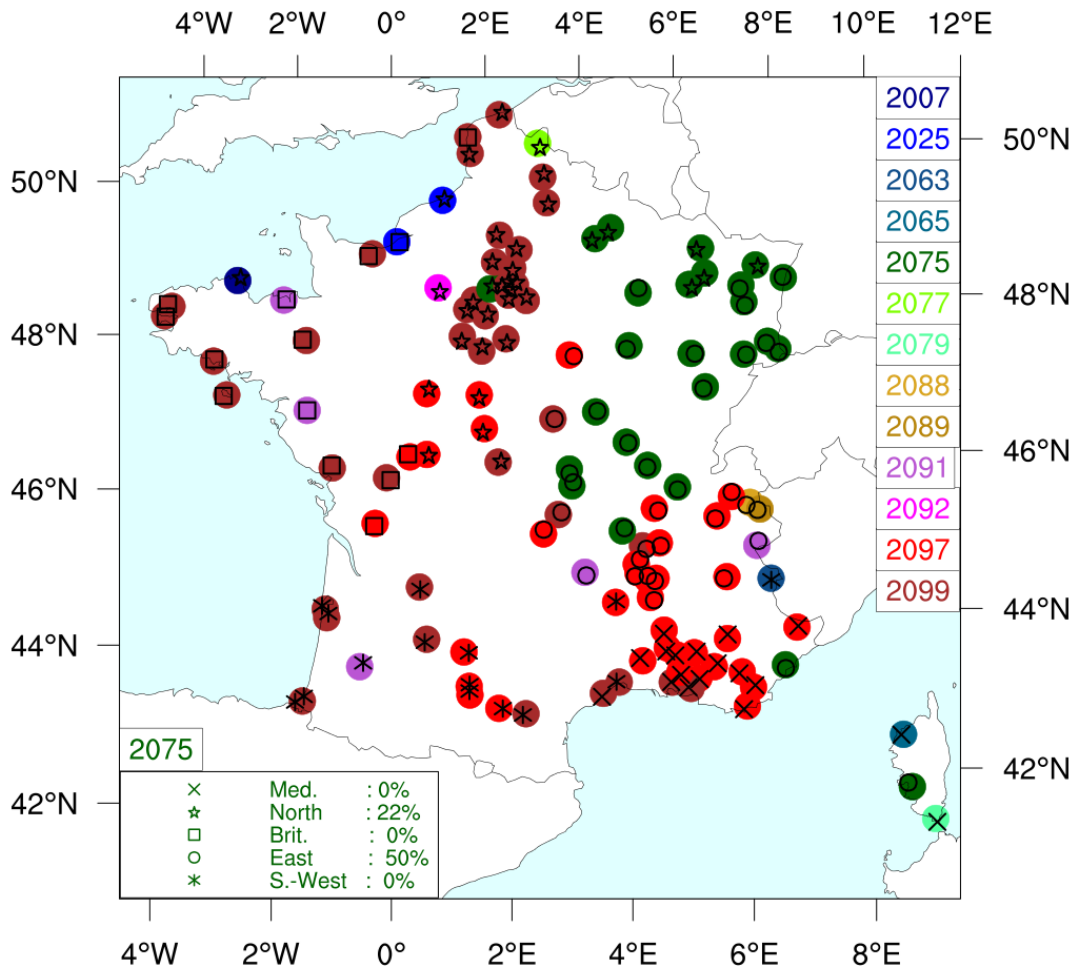
Figure S4: Spatial distribution of Tmax (°C) anomalies relative to the 2061-2090 climatology and averaged during the duration of the 2075 heatwave (days 192-221; see figure 4) in **(a)** the CNRM-CM5 simulation, **(b)** the ALADIN-SCEN simulation, and **(c)** the mean and **(d)** standard deviation of the 20-member ALADIN-LE simulations.
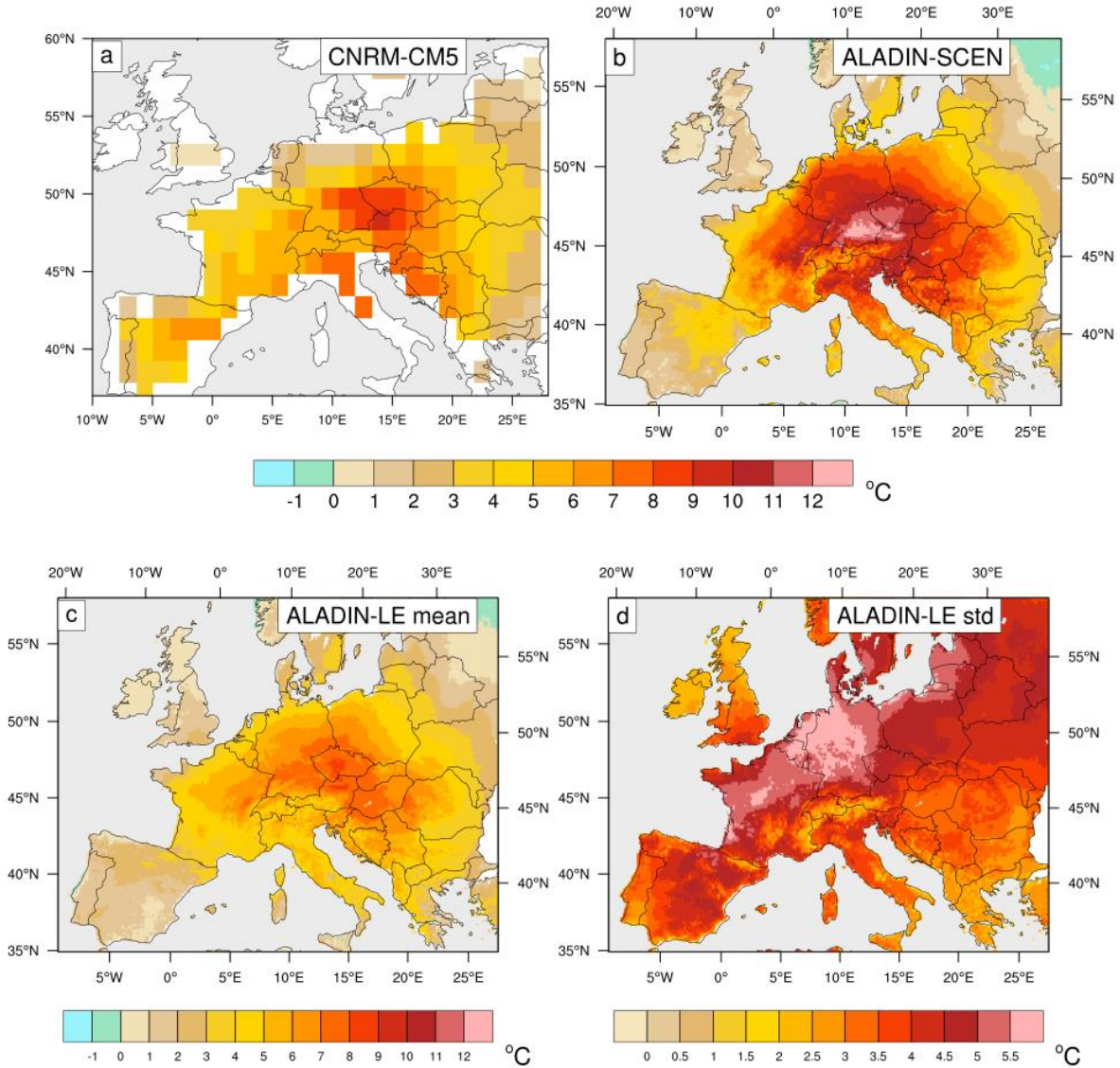
Figure S5: Daily evolution of the 500hPa geopotential height (m; in colors) and winds (m.s^{-1}; in contours) anomalies (relative to 2061-2090) during summer 2075 in the CNRM-CM5 simulation. The anomalies are averaged during moving 10-day periods showing the atmospheric conditions before, during (days 192-221; resumed in the last panel) and after the 2075 heatwave.